

Applications of Advanced Statistics to Astronomy

1. Application of the Fisher Information Matrix

Recall

$$\vec{x} \sim p(\vec{x} | \vec{\theta}) \text{ with } \vec{x} \in \mathbb{R}^n, \vec{\theta} \in \mathbb{R}^k$$

$$F_{ij}(\vec{\theta}^*) \equiv -\mathbb{E} \left[\frac{\partial^2 \ln p(\vec{x} | \vec{\theta})}{\partial \theta_i \partial \theta_j} \Bigg|_{\vec{\theta}=\vec{\theta}^*} \right] \text{ for } i, j \in \{1, \dots, k\}$$

$$\sqrt{n}(\hat{\vec{\theta}} - \vec{\theta}^*) \sim \mathcal{N} \left[0, F^{-1}(\vec{\theta}^*) \right]$$

$$\sigma_{\theta_i}^2 = n^{-1}(F^{-1})_{ii} : \text{marginalized error}$$

Fishing for Planets: A Comparative Analysis of EPRV Survey Performance in the Presence of Correlated Noise

ARVIND F. GUPTA ^{1, 2} AND MEGAN BEDELL  ³

¹*Department of Astronomy & Astrophysics, 525 Davey Laboratory, The Pennsylvania State University, University Park, PA, 16802,*

²*Center for Exoplanets and Habitable Worlds, 525 Davey Laboratory, The Pennsylvania State University, University Park, PA, 16802, USA*

³*Center for Computational Astrophysics, Flatiron Institute, 162 5th Avenue, New York, NY 10010, USA*

Submitted to AJ

ABSTRACT

With dedicated exoplanet surveys underway for multiple extreme precision radial velocity (EPRV) instruments, the near-future prospects of RV exoplanet science are promising. These surveys' generous time allocations are expected to facilitate the discovery of Earth analogs around bright, nearby Sun-like stars. But survey success will depend critically on the choice of observing strategy, which will determine the survey's ability to mitigate known sources of noise and extract low-amplitude exoplanet signals. Here, we present an analysis of the Fisher information content of simulated EPRV surveys, accounting for the most recent advances in our understanding of stellar variability on both short and long timescales (i.e., oscillations and granulation within individual nights, and activity-induced variations across multiple nights). In this analysis, we capture the correlated nature of stellar variability by parameterizing these signals with Gaussian Process kernels. We describe the underlying simulation framework as well as the physical interpretation of the Fisher information content, and we evaluate the efficacy of EPRV survey strategies that have been presented in the literature. We explore and compare strategies for scheduling observations over various timescales and we make recommendations to optimize survey performance for the detection of Earth-like exoplanets.

Keywords: Exoplanet Detection Methods – Radial Velocity – Surveys – Fisher Information – Stellar Activity

$\vec{x} \sim \mathcal{N}(\vec{\mu}, \mathbf{C})$: the radial velocity (RV) of an exoplanet

$$p(\vec{x}) = \frac{1}{(2\pi \det |\mathbf{C}|)^{N/2}} \exp \left[-\frac{1}{2} (\vec{x} - \vec{u})^t \mathbf{C}^{-1} (\vec{x} - \vec{u}) \right]$$

$$\vec{x}(t) = \{x(t_i)\}_{i=1}^N = \begin{pmatrix} x(t_1) \\ \vdots \\ x(t_N) \end{pmatrix} \quad \vec{\mu}(t) = \{\mu(t_i)\}_{i=1}^N = \begin{pmatrix} \mu(t_1) \\ \vdots \\ \mu(t_N) \end{pmatrix}$$

For our model in this work, we assume circular, zero-eccentricity orbits and single-planet systems such that the exoplanet-induced RV signal can be represented with a simplified Keplerian

$$\mu(t) = K \sin\left(\frac{2\pi}{P}t - \phi_0\right),$$

initial phase offset

period

$$\vec{\theta} = (K, P, \phi_0)^T$$

$$K = \frac{M_p \sin i}{\sqrt{1 - e^2}} \left(\frac{2\pi G}{(M_\star + M_p)^2 (P)} \right)^{1/3}.$$

star mass

planet mass

$$B_{i,j} = -\frac{\partial^2 \ln \mathcal{L}}{\partial \theta_i \partial \theta_j}$$

$$\begin{aligned} \ln \mathcal{L} = & -\frac{1}{2} \left[(x - \mu)^T C^{-1} (x - \mu) \right. \\ & \left. + N \ln 2\pi + \ln \det C \right] \end{aligned}$$

for a model μ and time series x of length N , and a $N \times N$ covariance matrix, C , that describes the expected noise properties of the measurements. Both μ and C may depend on θ in the general case.

In the case that the model parameters are independently Gaussianly distributed, the Fisher information can be written as

$$B_{i,j} = \left(\frac{\partial \mu}{\partial \theta_i} \right)^T C^{-1} \left(\frac{\partial \mu}{\partial \theta_j} \right) + \frac{1}{2} \text{tr} \left(C^{-1} \frac{\partial C}{\partial \theta_i} C^{-1} \frac{\partial C}{\partial \theta_i} \right) \quad (3)$$

or if the covariance is independent of the model parameters, simply

$$B_{i,j} = \left(\frac{\partial \mu}{\partial \theta_i} \right)^T C^{-1} \left(\frac{\partial \mu}{\partial \theta_j} \right). \quad (4)$$

The diagonal elements of the inverse of the Fisher information matrix represent the parameter uncertainties:

$$\sigma_{\theta_i}^2 = B_{i,i}^{-1}. \quad (5)$$

It is important to note here that the time series x has dropped out of the equation, and the Fisher information depends only on the model μ , the covariance matrix C , and the times t at which measurements are taken. That is, we do not need to know the measured values of x to determine the expected parameter uncertainties.

$$\frac{\partial \mu}{\partial \theta} = \begin{bmatrix} \frac{\partial \mu}{\partial K} \\ \frac{\partial \mu}{\partial P} \\ \frac{\partial \mu}{\partial \phi_0} \end{bmatrix} = \begin{bmatrix} \sin(\frac{2\pi}{P}t - \phi_0) \\ -\frac{2\pi t}{P^2}K \cos(\frac{2\pi}{P}t - \phi_0) \\ -K \cos(\frac{2\pi}{P}t - \phi_0) \end{bmatrix}$$

In a pure white noise scenario,

C will be a matrix with elements $C_{n,m} = \sigma_n^2 \delta_{nm}$, where σ_n is the total measurement uncertainty for observation $1 \leq n \leq N$ and δ is the delta function

$$\delta_{nm} = \begin{cases} 1 & m = n \\ 0 & m \neq n \end{cases}. \quad (10)$$

The full covariance matrix to be used in Equation 4 will be made up of a sum of white noise and correlated noise components

$$C = \sigma_{\text{photon}}^2 I + k_{\text{osc}} + k_{\text{gran}} + k_{\text{activity}}, \quad (11)$$

where I is the $N \times N$ identity matrix and the remaining terms are described below.

$$k_{\text{osc}}(\Delta) = S_{\text{osc}} \omega_{\text{osc}} Q e^{\frac{-\omega_{\text{osc}} \Delta}{2Q}} \times \left(\cos(\eta \omega_{\text{osc}} \Delta) + \frac{1}{2\eta Q} \sin(\eta \omega_{\text{osc}} \Delta) \right), \quad (12)$$

where Δ is the $N \times N$ matrix that represents the absolute value of the time delay between pairs of observations

$$\Delta_{n,m} = |t_n - t_m|. \quad (13)$$

$$k_{\text{gran}}(\Delta) = S_1 \omega_1 e^{\frac{-\omega_1 \Delta}{\sqrt{2}}} \cos \left(\frac{\omega_1 \Delta}{\sqrt{2}} - \frac{\pi}{4} \right) + S_2 \omega_2 e^{\frac{-\omega_2 \Delta}{\sqrt{2}}} \cos \left(\frac{\omega_2 \Delta}{\sqrt{2}} - \frac{\pi}{4} \right), \quad (14)$$

$$k_{\text{activity},QP}(\Delta) = \alpha^2 \exp \left(-\frac{\Delta^2}{2\lambda_1^2} - \Gamma \sin^2 \left(\frac{\pi \Delta}{\lambda_2} \right) \right) \quad (15)$$

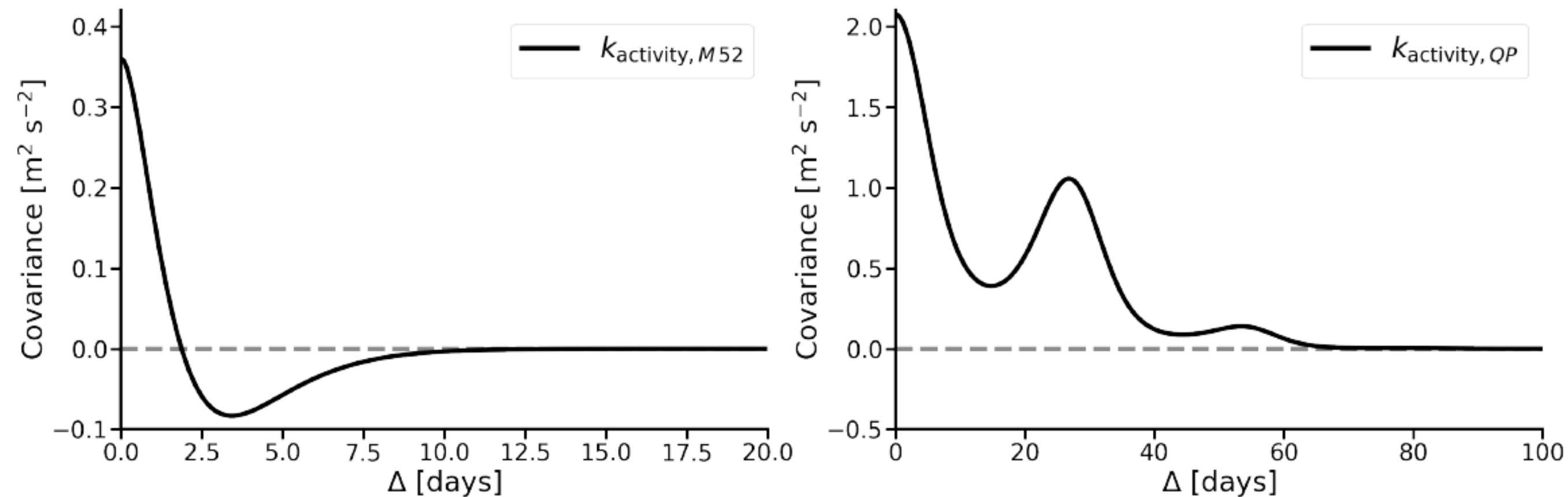


Figure 2. Covariance between pairs of observations as a function of separation in time for the quasiperiodic kernel for rotationally-modulated stellar activity (Equation 15; left) and for the Matern-5/2 kernel for rotationally-modulated stellar activity (Equation 16; right). While the covariance for both kernels persists across many nights, we note that the curves differ significantly in amplitude and shape.

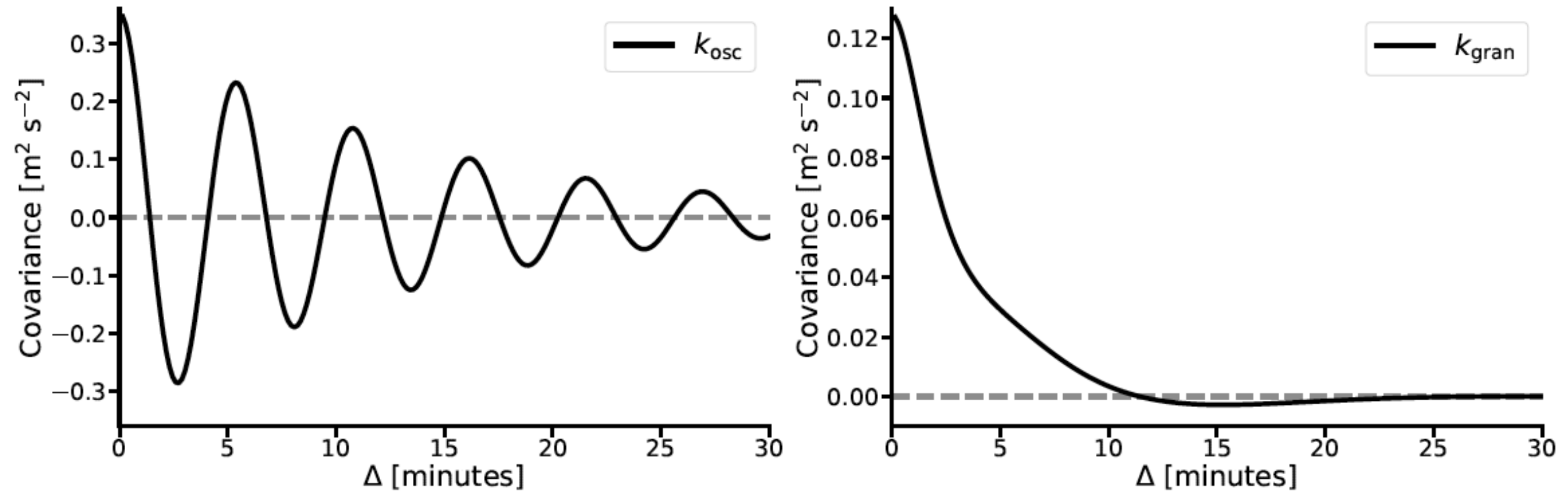
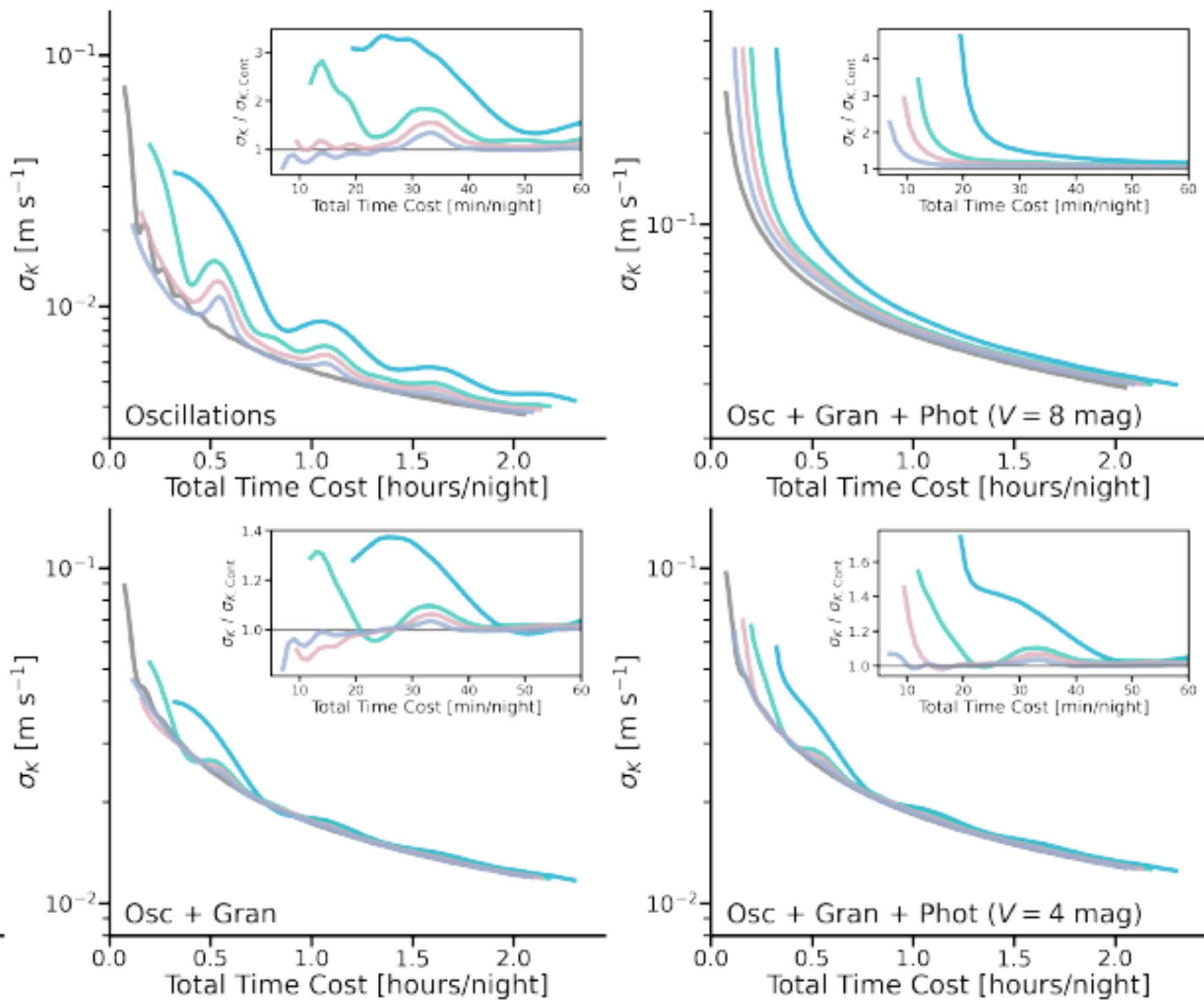
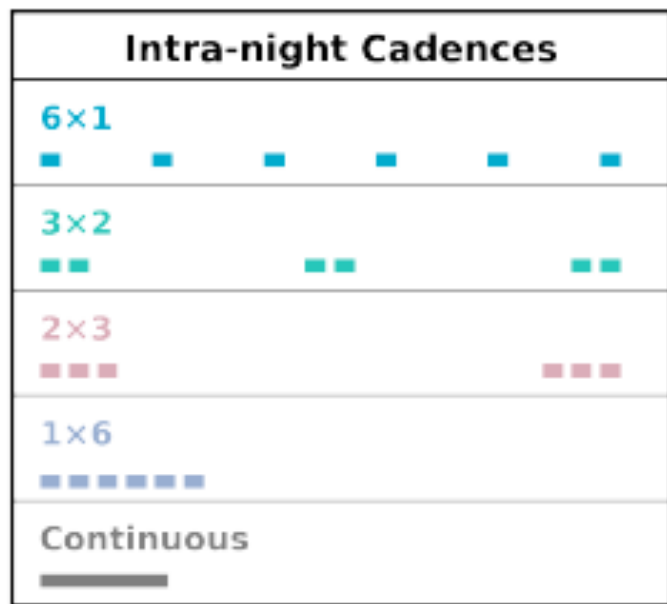
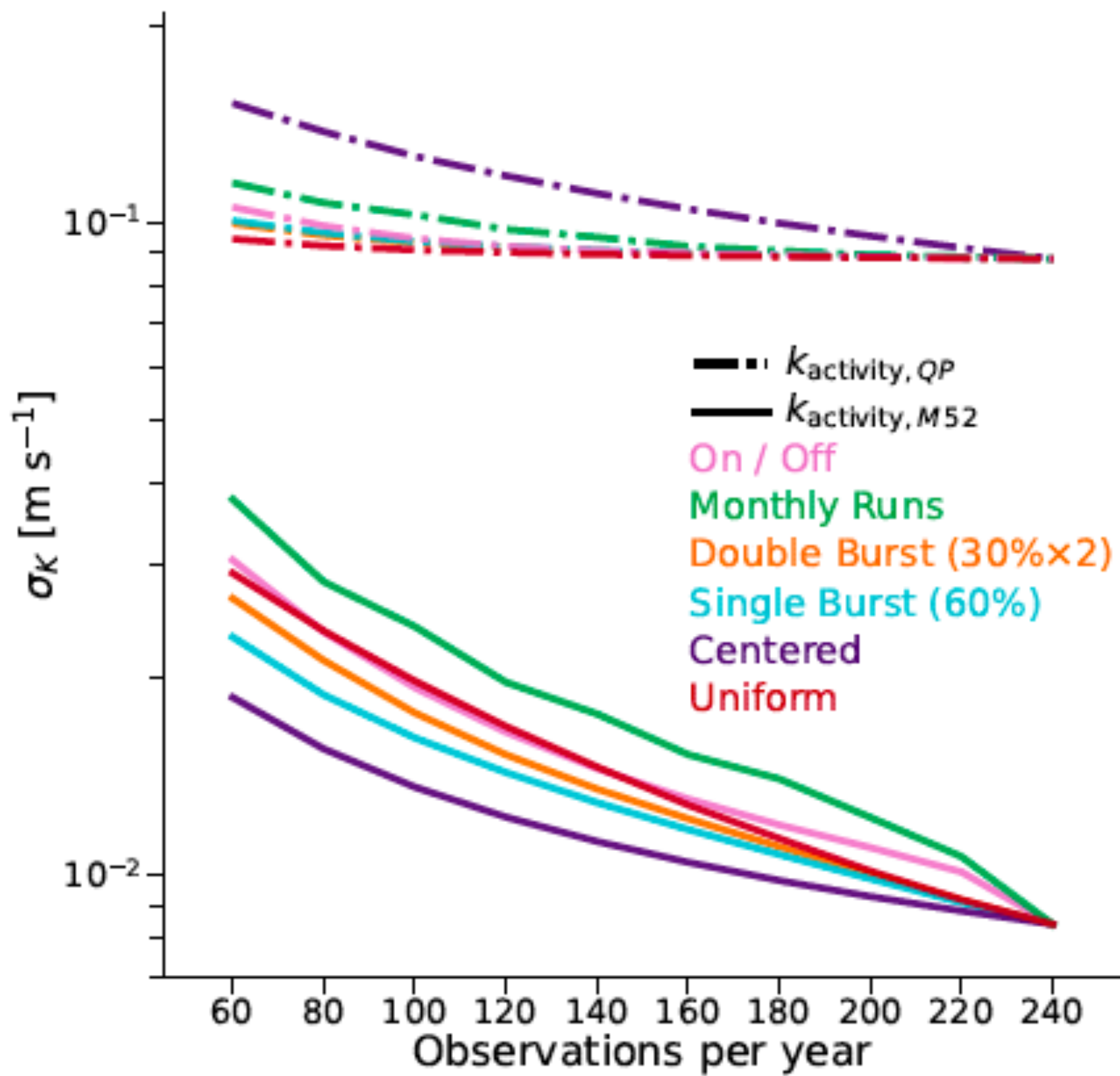


Figure 1. Covariance between pairs of observations as a function of separation in time for the GP kernels for stellar oscillations (Equation 12; left) and for stellar surface granulation (Equation 14; right). We assume instantaneous exposures for both kernels. We show that oscillations and granulation only introduce significant RV noise on short timescales of less than a single night.





2. Application of the Wiener Filter (WF)

Recall

$$\vec{X} = \vec{S} + \vec{W}, \vec{S} \sim \mathcal{N}(\vec{0}, \Sigma_{ss}), \vec{W} \sim \mathcal{N}(\vec{0}, \Sigma_{ww})$$

- The Wiener filter is given as:

$$\Sigma_{sx}\Sigma_{xx}^{-1} = \Sigma_{ss}\Sigma_{xx}^{-1} = \Sigma_{ss} (\Sigma_{ss} + \Sigma_{ww})^{-1}$$

- The signal can be reconstructed as:

$$\hat{\vec{s}} = \Sigma_{sx}\Sigma_{xx}^{-1} = \Sigma_{ss}\Sigma_{xx}^{-1} = \Sigma_{ss} (\Sigma_{ss} + \Sigma_{ww})^{-1} \vec{x}$$

The 2dF Galaxy Redshift Survey: Wiener reconstruction of the cosmic web

Pirin Erdoğdu,^{1,2}★ Ofer Lahav,^{1,18} Saleem Zaroubi,³ George Efstathiou,¹ Steve Moody,
John A. Peacock,¹² Matthew Colless,¹⁷ Ivan K. Baldry,⁹ Carlton M. Baugh,¹⁶
Joss Bland-Hawthorn,⁷ Terry Bridges,⁷ Russell Cannon,⁷ Shaun Cole,¹⁶ Chris Collins,⁴
Warrick Couch,⁵ Gavin Dalton,^{6,15} Roberto De Propris,¹⁷ Simon P. Driver,¹⁷
Richard S. Ellis,⁸ Carlos S. Frenk,¹⁶ Karl Glazebrook,⁹ Carole Jackson,¹⁷ Ian Lewis,⁶
Stuart Lumsden,¹⁰ Steve Maddox,¹¹ Darren Madgwick,¹³ Peder Norberg,¹⁴
Bruce A. Peterson,¹⁷ Will Sutherland¹² and Keith Taylor⁸ (the 2dFGRS Team)

¹Institute of Astronomy, Madingley Road, Cambridge CB3 0HA

²Department of Physics, Middle East Technical University, 06531, Ankara, Turkey

³Kapteyn Institute, University of Groningen, PO Box 800, 9700 AV, Groningen, the Netherlands

⁴Astrophysics Research Institute, Liverpool John Moores University, Twelve Quays House, Birkenhead L14 1LD

⁵Department of Astrophysics, University of New South Wales, Sydney, NSW 2052, Australia

⁶Department of Physics, University of Oxford, Keble Road, Oxford OX1 3RH

⁷Anglo-Australian Observatory, PO Box 296, Epping, NSW 2111, Australia

⁸Department of Astronomy, California Institute of Technology, Pasadena, CA 91025, USA

⁹Department of Physics and Astronomy, Johns Hopkins University, Baltimore, MD 21118-2686, USA

¹⁰Department of Physics, University of Leeds, Woodhouse Lane, Leeds LS2 9JT

¹¹School of Physics and Astronomy, University of Nottingham, Nottingham NG7 2RD

¹²Institute for Astronomy, University of Edinburgh, Royal Observatory, Blackford Hill, Edinburgh EH9 3HJ

¹³Lawrence Berkeley National Laboratory, 1 Cyclotron Road, Berkeley, CA 94720, USA

¹⁴ETHZ Institut für Astronomie, HPF G3.1, ETH Hönggerberg, CH-8093 Zurich, Switzerland

¹⁵Rutherford Appleton Laboratory, Chilton, Didcot OX11 0QX

¹⁶Department of Physics, University of Durham, South Road, Durham DH1 3LE

¹⁷Research School of Astronomy and Astrophysics, The Australian National University, Weston Creek, ACT 2611, Australia

¹⁸Department of Physics and Astronomy, University College London, Gower Street, London WC1E 6BT

Let us assume that we have a set of measurements, $\{d_\alpha\}$ ($\alpha = 1, 2, \dots, N$) which are a linear convolution of the true underlying signal, s_α , plus a contribution from statistical noise, ϵ_α , such that

$$d_\alpha = \underbrace{s_\alpha}_{\delta \equiv (\rho - \bar{\rho})/\bar{\rho}} + \epsilon_\alpha.$$

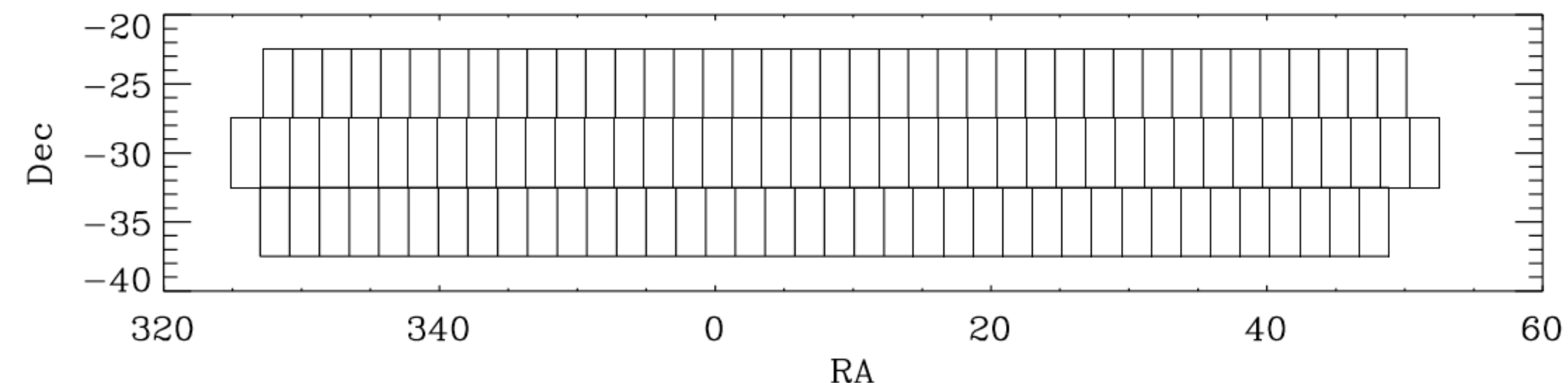
It is straightforward to show that the Wiener filter is

$$F_{\alpha\beta} = \langle s_\alpha d_\gamma^\dagger \rangle \langle d_\gamma d_\beta^\dagger \rangle^{-1},$$

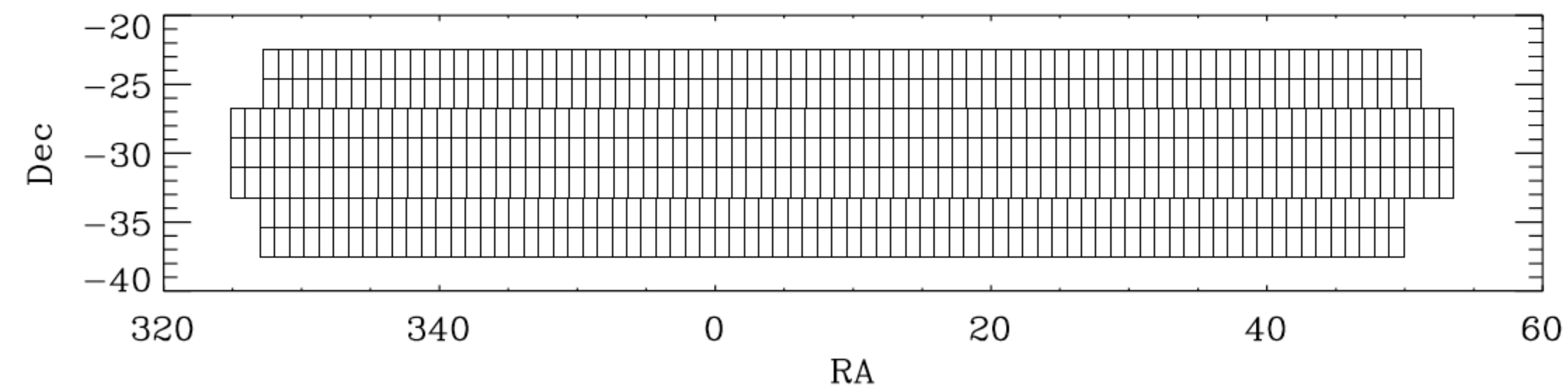
$$\langle s_\alpha d_\gamma^\dagger \rangle = \langle s_\alpha s_\gamma^\dagger \rangle, \quad \langle d_\alpha d_\beta^\dagger \rangle = \langle s_\gamma s_\delta^\dagger \rangle + \langle \epsilon_\alpha \epsilon_\beta^\dagger \rangle.$$

$$\mathbf{s}^{\text{WF}} = \mathbf{C} [\mathbf{C} + \mathbf{N}]^{-1} \mathbf{d}.$$

SGP $0.050 < z < 0.054$



SGP $0.049 < z < 0.051$



data vector \mathbf{d} as

$$d_i = \frac{N_i - \bar{N}_i}{\bar{N}_i}.$$

the volume
of the pixel

$$\bar{N}_i = \bar{n} V_i,$$

the mean galaxy density

$$N_i = \sum_{\text{gal}}^{N_{\text{gal}}(i)} w(\text{gal})$$

:

the number of galaxies
in each pixel i

where the sum is over all the observed galaxies
in the pixel and $w(\text{gal})$ is the weight assigned
to each galaxy

$$w(\text{gal}) = \frac{1}{\phi(z_{\text{gal}}) M(\Omega_i)}$$

selection function

angular survey mask

The selection function can be expressed as

$$\phi(r) = \frac{\int_{L(r)}^{\infty} \Phi(L) dL}{\int_{L_{\min}}^{\infty} \Phi(L) dL}$$

the probability of observing a galaxy for a given redshift

where $\Phi(L)$ is the galaxy luminosity function:

$$\Phi(L) dL = \Phi^* \left(\frac{L}{L^*} \right)^\alpha \exp \left(-\frac{L}{L^*} \right) \frac{dL}{L^*}.$$

$L(r)$: the minimum luminosity detectable

$L_{\min} = \text{Min}[L(r), L_{\text{com}}]$

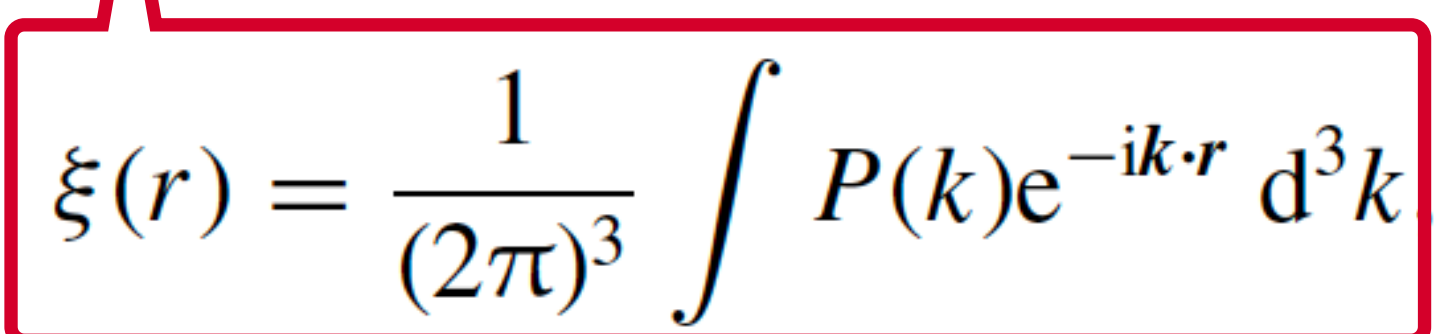
L_{com} : the minimum luminosity for which the catalogue is complete

The signal covariance matrix can be accurately modelled by an analytical approximation (Moody 2003). The calculation of

$$\langle C_{ij} \rangle = \left\langle \frac{1}{V_i V_j} \int_{\text{Cell}_i} \delta(\mathbf{x}) dV_i \int_{\text{Cell}_j} \delta(\mathbf{x} + \mathbf{r}) dV_j \right\rangle$$

$$= \frac{1}{V_i V_j} \int_{\text{Cell}_i} \int_{\text{Cell}_j} \langle \delta(\mathbf{x}) \delta(\mathbf{x} + \mathbf{r}) \rangle dV_i dV_j$$

$$= \frac{1}{V_i V_j} \int_{\text{Cell}_i} \int_{\text{Cell}_j} \xi(\mathbf{r}) dV_i dV_j$$



$$\xi(r) = \frac{1}{(2\pi)^3} \int P(k) e^{-ik \cdot r} d^3 k$$

$$\langle C_{ij} \rangle = \frac{1}{(2\pi)^3 V_i V_j} \int P(k) d^3k \int_{\text{Cell}_i} \int_{\text{Cell}_j} e^{-ik(r_i - r_j)} dV_i dV_j.$$

After performing the Fourier transform,

$$C(\mathbf{k}, \mathbf{r}) = \cos(k_x r_x) \cos(k_y r_y) \cos(k_z r_z).$$

$$\langle C_{ij} \rangle = \frac{1}{(2\pi)^3} \int P(k) S(\mathbf{k}, \mathbf{L}_i) S(\mathbf{k}, \mathbf{L}_j) C(\mathbf{k}, \mathbf{r}) d^3k,$$

$$S(\mathbf{k}, \mathbf{L}) = \text{sinc}(k_x L_x/2) \text{sinc}(k_y L_y/2) \text{sinc}(k_z L_z/2)$$

$$\text{sinc}(x) = (\sin(x))/x$$

\mathbf{L} describes the dimensions of the cell (L_x, L_y, L_z)

correlation matrix \mathbf{C} formulated in the previous section. The only change made is to the calculation of \mathbf{C} where the real-space correlation function $\xi(r)$ is now multiplied by the Kaiser factor in order to correct for the redshift distortions on large scales. So

$$\xi_s = \frac{1}{(2\pi)^3} \int P^S(k) \exp[i\mathbf{k} \cdot (\mathbf{r}_2 - \mathbf{r}_1)] d^3k,$$

where $P^S(k)$ is the galaxy power spectrum in redshift space

$$P^S(k) = K[\beta] P^R(k).$$

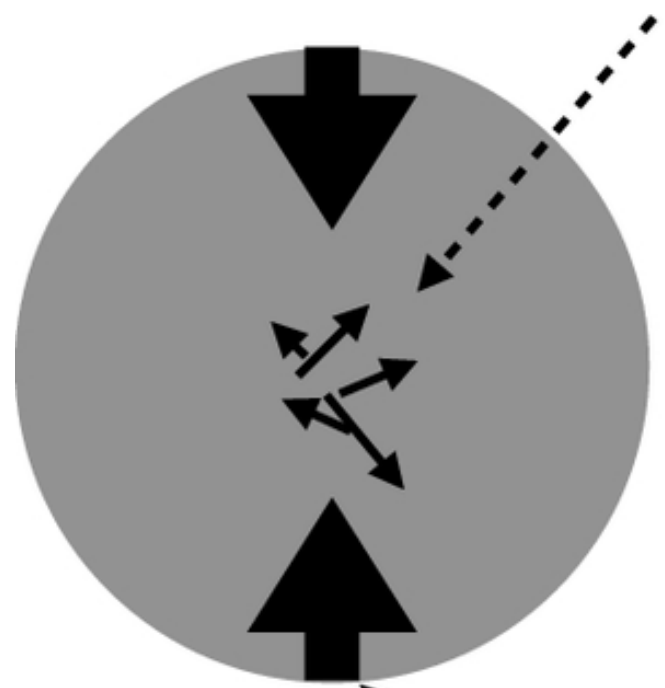
$$K[\beta] = 1 + \frac{2}{3}\beta + \frac{1}{5}\beta^2$$

direction averaged
Kaiser factor

$$\beta \equiv \Omega_m^{0.6}/b$$

redshift distortion factor

Real space

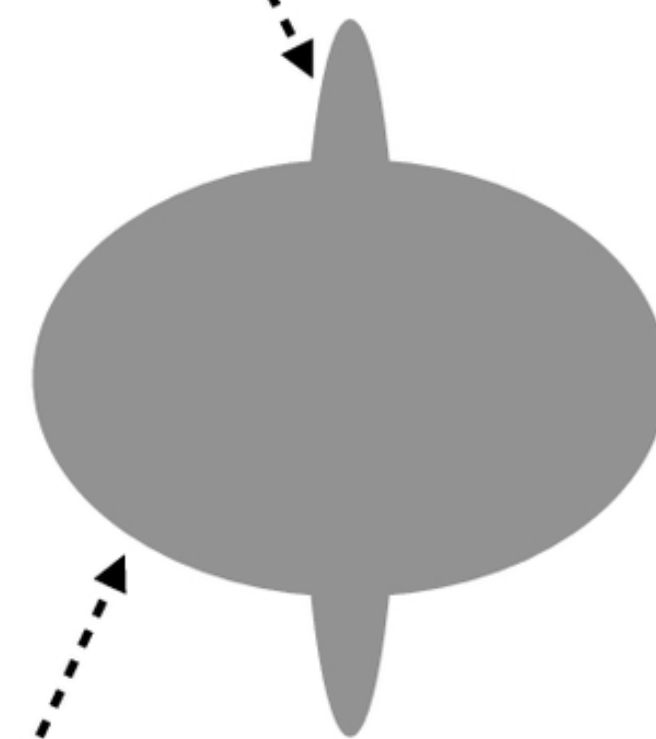


Small-scale
motions



Redshift space

"Fingers of God"
effect



Large-scale
infall



Kaiser
effect

Line
of
sight

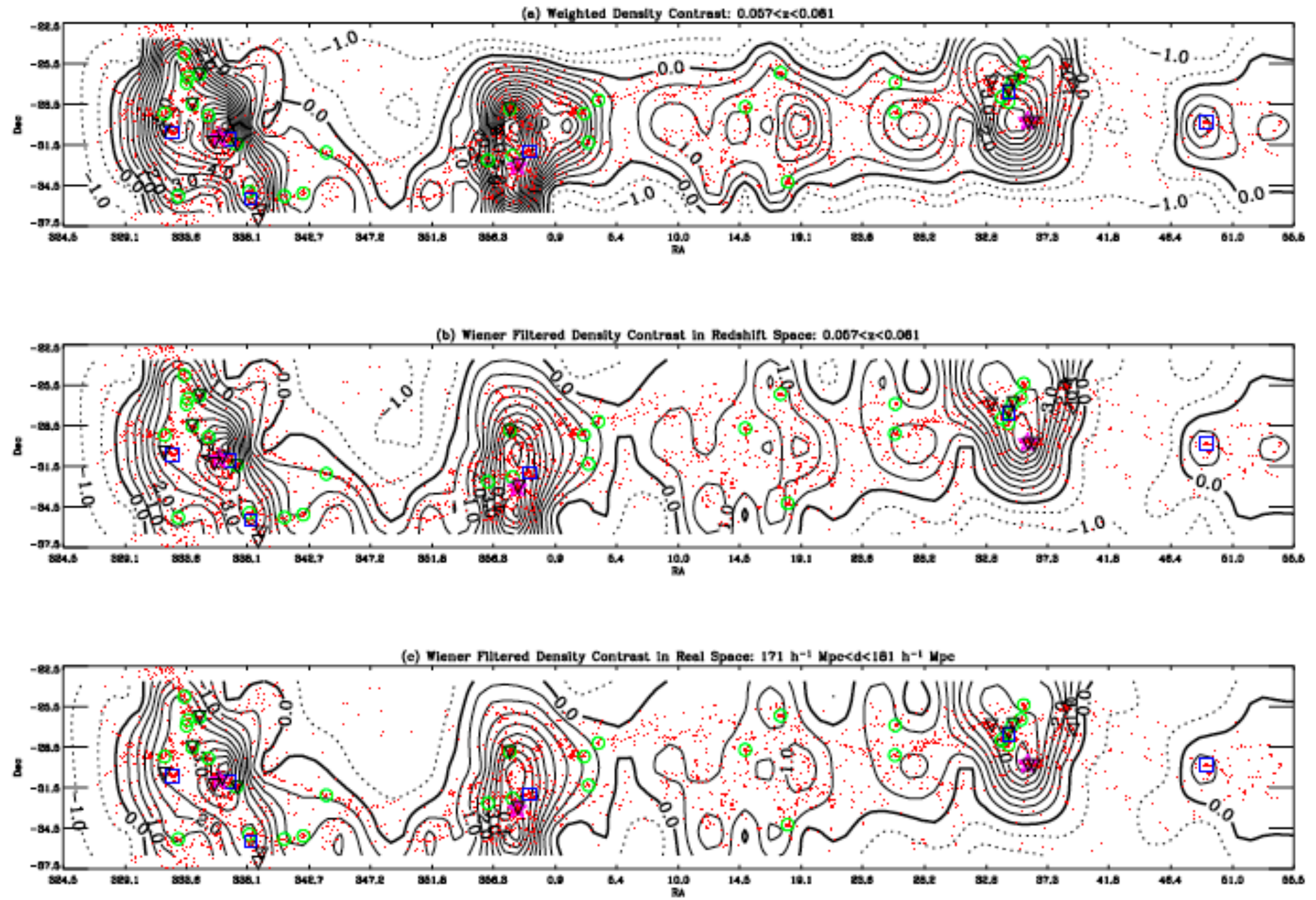


$$\langle s(\mathbf{r})d(\mathbf{s}) \rangle = \langle \delta_{\mathbf{r}} \delta_{\mathbf{s}} \rangle = \xi(r) \left(1 + \frac{1}{3} \beta \right)$$

$$s^{\text{WF}}(\mathbf{r}) = \frac{1 + (1/3)\beta}{K[\beta]} \mathbf{C} [\mathbf{C} + \mathbf{N}]^{-1} \mathbf{d}.$$

noise correlation matrix \mathbf{N} . Assuming that the noise in different cells is not correlated, the only non-zero terms in \mathbf{N} are the diagonal terms given by the variance – the second central moment – of the density error in each cell:

$$\mathcal{N}_{ii} = \frac{1}{\bar{N}_i^2} \sum_{\text{gal}}^{N_{\text{gal}}(i)} w^2(\text{gal}).$$



Reconstructions of the 2dFGRS SGP region for the redshift range $0.057 \leq z \leq 0.061$ for $10 \text{ } h^{-1} \text{ Mpc}$ target cell size. The contours are spaced at $\Delta\delta = 0.5$ with solid (dashed) lines denoting positive (negative) contours

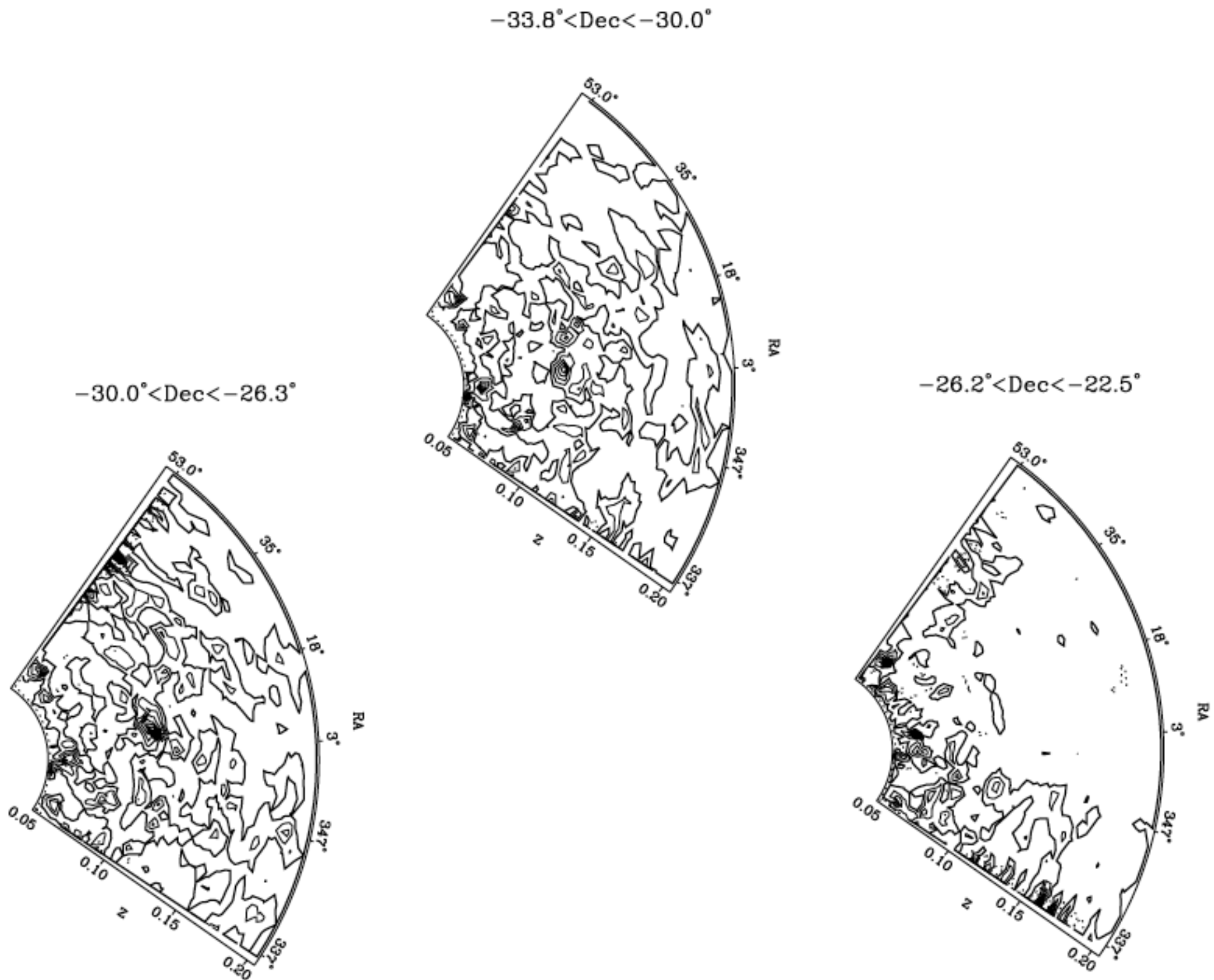


Figure 7. Reconstructions of the 2dFGRS SGP region in slices of declination for $10 h^{-1} \text{ Mpc}$ target cell size. The declination range is given on the top of each plot. The contours are spaced at $\Delta\delta = 1.0$ with solid (dashed) lines denoting positive (negative) contours; the heavy solid contours correspond to $\delta = 0$.